4 Lecture 4: Heteroclinic cycles and networks

4.1 Introduction

A heteroclinic orbit γ_1 between two equilibria ξ_1 and ξ_2 of a continuous time dynamical system $\dot{x} = f(x)$ is a trajectory $\phi_t(y)$ that is backward asymptotic to ξ_1 and forward asymptotic to ξ_2. A heteroclinic cycle is an invariant topological circle X consisting of the union of a set of equilibria $\{\xi_1, ..., \xi_k\}$ and orbits $\{\gamma_1, ..., \gamma_k\}$, where γ_i is a heteroclinic orbit between ξ_i and ξ_{i+1}; and $\xi_{k+1} \equiv \xi_1$. If $k = 1$ then the single equilibrium and connecting orbit form a homoclinic cycle.

For a typical dynamical system (without symmetry), heteroclinic cycles are extremely unlikely. However, if the heteroclinic orbits lie in invariant subspaces, the cycle can be robust (i.e. persistent) under perturbations of the system that preserve the invariance of these subspaces. This situation can arise if the dynamical system is symmetric (for example when it arises a a model of pattern formation), or if it models population (or game theory) dynamics, where extinction is a preserved quantity (for examples, refer to the book by Hofbauer and Sigmund [31]). This concept of robustness motivates the following definition: X is a robust heteroclinic cycle if for each j, $1 \leq j \leq k$ there exists a fixed point subspace, $P_j = \mathrm{Fix}(\Sigma_j)$ where $\Sigma_j \subset \mathcal{G}$ and

1. ξ_j is a saddle and ξ_{j+1} is a sink in P_j
2. there is a heteroclinic connection from ξ_j to ξ_{j+1} in P_j

(indices are taken *mod* k). In some cases in the literature all equilibria ξ_j and connecting orbits lie on a single group orbit: then, after factoring out the symmetry, the cycle can be thought of as homoclinic rather than heteroclinic. In sections 4.2 and 4.3 we discuss two well-known examples of heteroclinic cycles. Later sections summarise recent work on cycles in $\mathbb{R}^4$, and an example in $\mathbb{R}^6$. A collection of heteroclinic cycles with equilibria in common forms a *heteroclinic network*: networks are discussed very briefly in the final section. A recommended general overview of the dynamics of robust cycles is the review by Krupa [36].

4.2 The $1:2$ mode interaction

The material in the section follows the paper by Proctor & Jones [45]. Among other papers on the very rich dynamics in this problem are those by Dangelmayr [13], Armbruster, Guckenheimer & Holmes [1], Julien [33], Porter & Knobloch [44] and Dawes, Postlethwaite & Proctor [16].

A mode interaction is a degenerate bifurcation at which there is a simultaneous instability to more than one type of perturbation. There are three basic kinds: where the competing instabilities are both steady-state, or one steady-state and one Hopf, or both Hopf. In the absence of symmetry or any special properties the steady-state bifurcation would be a saddle-node. The analysis of these codimension two bifurcations becomes quite involved: see Guckenheimer & Holmes [28], chapter 7. In the Hopf cases, the existence or absence of normal form symmetry is particularly important.

In the pattern formation context there is another factor in distinguishing between different codimension two instabilities: the wavenumbers of the instabilities matter as well as their nature (steady or oscillatory). Consider the simultaneous instability of a one dimensional spatially uniform state to two steady-state instabilities, as sketched in figure 12. To arrive at this situation we usually have to vary two independent control parameters. Near the onset of the instability we propose a solution of the form

$$w(x,t) \quad = \quad A(t)\mathrm{e}^{\mathrm{i}k_1 x} + B(t)\mathrm{e}^{\mathrm{i}k_2 x} + \text{c.c.} + \cdots .$$

By considering equivariance under translations in x, and reflection $m_x : x \to -x$

$$\begin{aligned} \tau_\phi(x) &= x - \phi \ ; & \tau_\phi(A,B) &= (A\mathrm{e}^{\mathrm{i}k_1\phi}, B\mathrm{e}^{\mathrm{i}k_2\phi}), \\ m_x(x) &= -x \ ; & m_x(A,B) &= (\bar{A}, \bar{B}), \end{aligned}$$

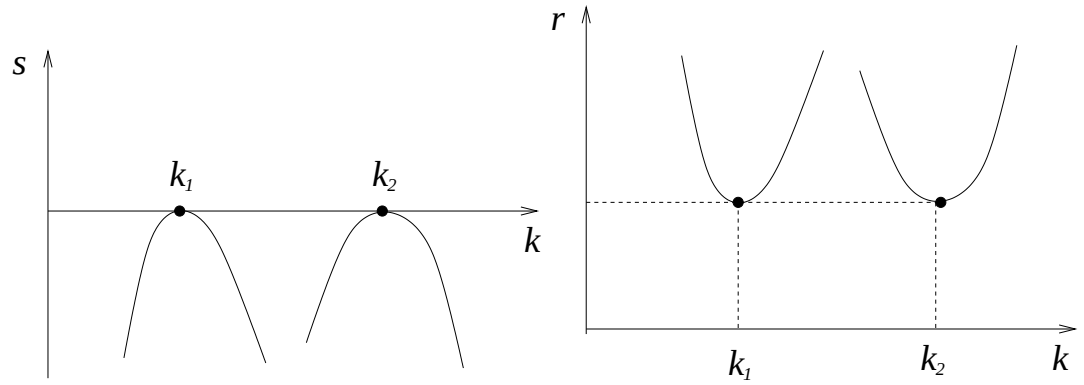

Figure 12: (a) Sketch of the (k, s) plane showing growth rate s (real) as as function of wavenumber k. (b) Sketch of the corresponding marginal stability curves $s(r, k) = 0$ in the (k, r) plane where r is a real control parameter for the system.

we arrive at the usual coupled amplitude equations:

$$\dot{A} = \mu_1 A - a_1 A|A|^2 - b_1 A|B|^2, \tag{35}$$
$$\dot{B} = \mu_2 B - a_2 B|B|^2 - b_2 B|A|^2, \tag{36}$$

where all coefficients are forced to be real by the reflection symmetry, as long as the wavenumbers k_1 and k_2 are not resonant. By resonant we mean that for one of the k_j (here, either $j = 1$ or 2) the equation $k_j = pk_1 + qk_2$ has non-trivial solutions for non-negative integers p and q. If there were such a solution then the RHS of the equations would contain more terms. Cases of resonance where $|p| + |q| \leq 3$ are termed 'strong resonances' since then new terms appear in (35) - (36) at quadratic or cubic order and they affect the bifurcation behaviour for small μ_1 and μ_2.

The $1 : 2$ mode interaction corresponds to the strong resonance case $k_1 = 1$, $k_2 = 2$ (take $j = 2$, $p = 2$, $q = 0$ in the resonance condition). From translational equivariance we see that terms $\bar{A}B$ and A^2 are now allowed on the RHS of (35) - (36). By rescaling we can set the coefficient of $\bar{A}B$ to be $+1$ and that of A^2 to be ± 1:

$$\dot{A} = \mu_1 A - a_1 A|A|^2 - b_1 A|B|^2 + \bar{A}B, \tag{37}$$
$$\dot{B} = \mu_2 B - a_2 B|B|^2 - b_2 B|A|^2 \pm A^2. \tag{38}$$

Note that there is a possible inconsistency in scalings here (if, say, we wished to derive these equations through an asymptotic multiple-scales calculation from the original PDEs). For consistency we should suppose that the original coefficients of the quadratic terms were 'small' compared to those of the cubic terms: we can then justify including both quadratic and cubic terms together in our amplitude equations.

In polar coordinates $A = Re^{i\theta}$, $B = Se^{i\phi}$ we have

$$\dot{R} = R(\mu_1 - a_1 R^2 - b_1 S^2) + RS\cos\chi, \tag{39}$$
$$\dot{S} = S(\mu_2 - a_2 S^2 - b +_2 R^2) \pm R^2 \cos\chi, \tag{40}$$
$$\dot{\chi} = \left(\mp\frac{R^2}{S} - 2S\right)\sin\chi. \tag{41}$$

Only one phase variable $\chi = \phi - 2\theta$ is important: this is due to the translational symmetry. It turns out that the two cases given by the choice of $\pm$ in (40) give very different bifurcation diagrams. The '+' case displays far less interesting dynamics than the '$-$' case. Interestingly, the '$-$' case is

the one that occurs regularly in fluid-mechanical situations, so fluid mechanics (in particular the nonlinear Navier–Stokes term $\mathrm{u} \cdot \nabla \mathrm{u}$) is inherently 'interesting' (!)

From now on we will focus exclusively on the '$-$' case.

Equilibria

- Trivial eqm $A = B = 0$, stable in $\mu_1 < 0$, $\mu_2 < 0$
- 'Pure mode' eqm $A = 0$, $|B|^2 = \mu_2/a_2$. This is a circle of equilibria: a group orbit under the translation symmetry. Denote the two equilibria corresponding to A, B real by $p_\pm$: $A = 0$, $B = \pm\sqrt{\mu_2/a_2}$.

  It is easy to check that $p_\pm$ lose stability when $0 = \mu_1 - \frac{b_1}{a_2}\mu_2 \pm \sqrt{\frac{\mu_2}{a_2}}$
- 'Mixed mode' solutions $M_\pm$ satisfy $|A| \neq 0$, $|B| \neq 0$ and hence $\chi = 0$ (M_+) or $\chi = \pi$ (M_-) from (41). Amplitudes $R = |A|$ and $S = |B|$ satisfy

$$\begin{aligned} 0 &= \mu_1 \pm S - a_1 R^2 - b_1 S^2, \\ o &= \mu_2 S \mp R^2 - a_2 S^3 - b_2 R^2 S, \end{aligned}$$

  where the $\pm$ and $\mp$ refer to $M_\pm$ respectively. There exists a continuous group orbit of each of $M_\pm$: they have entirely different stabilities (and physical interpretations) from each other though.

Bifurcations from M_+

M_+ loses stability in two different ways. Firstly a Hopf bifurcation is possible when

$$2a_1 R^2 + 2a_2 S^2 = R^2/S$$

as long as

$$a_1(2a_2 S^2 - R^2/S) + (1 - 2b_1 S)(1 + b_2 S) \geq 0.$$

This Hopf bifurcation leads to a time-periodic oscillation of R and S but the phase $\chi = 0$ is constant. Hence this solution is a standing wave (SW). The second possibility is that $\chi \neq 0$ after the bifurcation. This leads to travelling waves (TW) for which $R^2 = 2S^2$ from (41), and

$$\begin{aligned} S^2 &= \frac{2\mu_1 + \mu_2}{4a_1 + 2(b_1 + b_2) + a_2}, \\ S\cos\chi &= \frac{\mu_2(2a_1 + b_1) - \mu_1(2b_2 + a_2)}{4a_1 + 2(b_1 + b_2) + a_2}. \end{aligned}$$

This is an example of a drift bifurcation since the TW state rotates along the group orbit of M_+ equilibria. Even though $\chi = \text{const}$ the individual phases θ and ϕ evolve at constant rates in time:

$$\begin{aligned} \dot{\phi} &= -2S\sin\chi \\ \dot{\theta} &= -S\sin\chi \end{aligned}$$

and in the (R, S, χ) coordinates TW solutions are equilibria. For typical parameter values the bifurcation diagram in the (μ_1, μ_2) plane looks like figure 13. For the parameter values of figure 13 the bifurcation to TW (on the line TW) is supercritical and that to SW (on the line SW) is subcritical. The global bifurcation marked *het* generates unstable SW periodic orbits which then collapse onto the M_+ equilibrium and disappear on the curve marked SW. The phase portrait sketches in figure 14 illustrate the bifurcations that lead to the formation of the heteroclinic cycle.

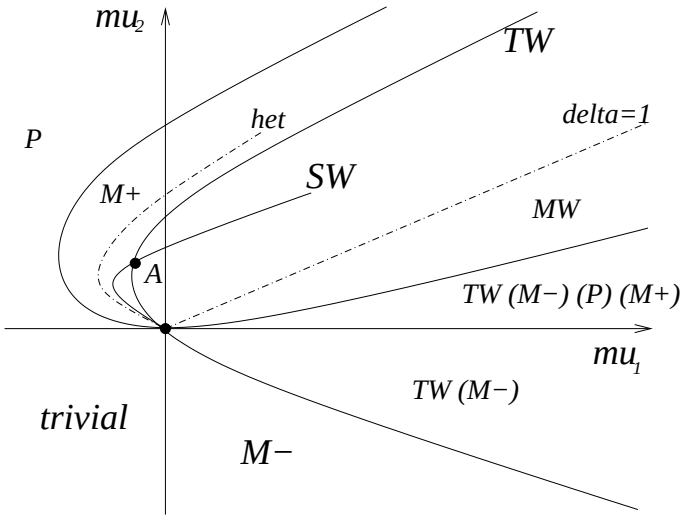

Figure 13: Typical bifurcation diagram for the $1:2$ mode interaction. Stable and unstable equilibria in each region of the parameter plane indicated (unstable solutions in parentheses ()). The robust heteroclinic cycle exists and is stable between curves marked *het* and *delta=1*. Between *delta=1* and the next solid line to the right the robust cycle exists but is unstable. $a_1 = 1$, $b_1 = 2$, $a_2 = 5$, $b_2 = 0$. Taken from Proctor & Jones [45].

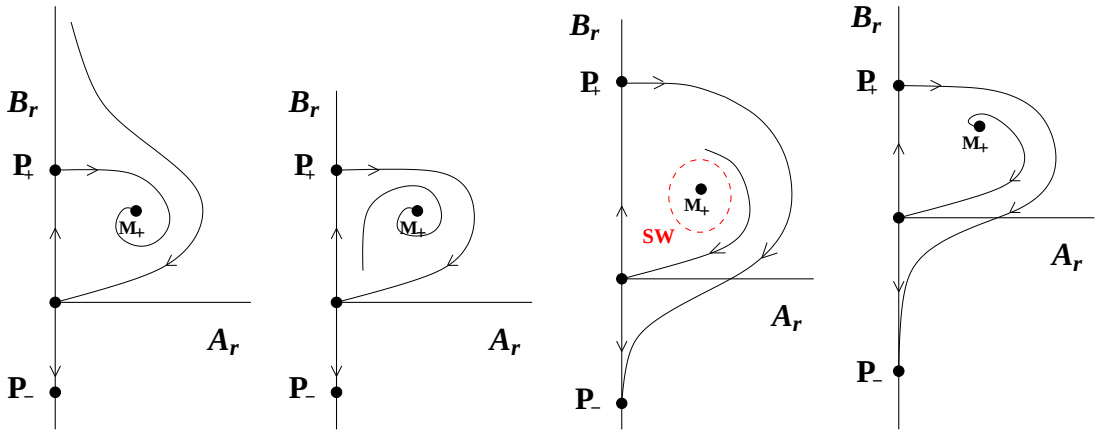

Figure 14: Phase portraits in the (A_r, B_r) plane (taking the real parts of A and B) for μ_1 increasing at fixed $\mu_2 > 0$. (a) left of the line *het*; (b) on the line *het*; (c) between the lines *het* and SW showing unstable SW periodic orbit and the robust heteroclinic connection $p_+ \to p_-$; (d) right of the line SW: the heteroclinic connection remains.

The heteroclinic connection $p_+ \to p_-$ is robust since p_- is a sink (stable node) within this plane, which is an invariant subspace $P_- = \mathrm{Fix}(m_x) = \{Im(A) = Im(B) = 0\}$ for the dynamics. By symmetry, within the plane $P_+ = \mathrm{Fix}(\tau_\pi \circ m_x) = \{Re(A) = Im(B) = 0\}$ p_- is a saddle and p_+ is a sink, and a symmetrically-related heteroclinic orbit $p_- \to p_+$ exists. The saddle-sink connections are not immediately broken as μ_1, μ_2 are varied so the cycle persists. For the parameter values given above it turns out that this heteroclinic cycle attracts nearby trajectories. The times that a trajectory spends near each equilibrium increase geometrically: $T_n/T_{n-1} \to C > 1$ as $n \to \infty$. The stability question can be investigated by similar 'return map' methods as is done for periodic orbits. The condition for the cycle to be attracting can then be calculated as $\delta \equiv |\lambda_c|/\lambda_e > 1$

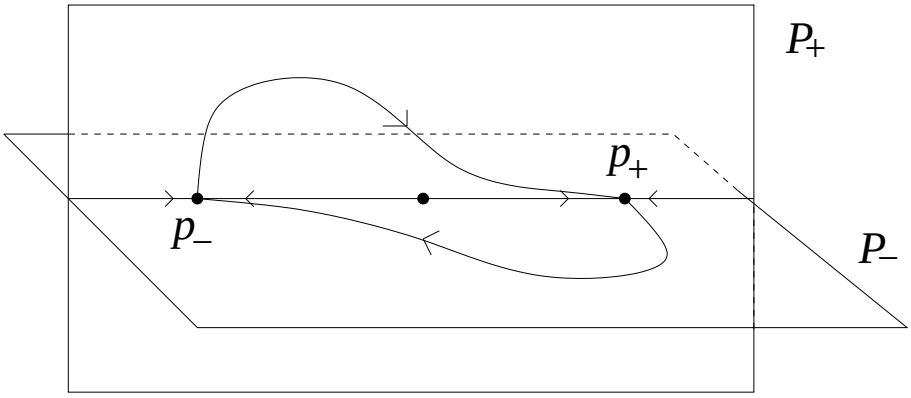

Figure 15: The heteroclinic cycle. $P_+ = \mathrm{Fix}(m_x) = \{Im(A) = Im(B) = 0\}$, $P_- = \mathrm{Fix}(\tau_\pi \circ m_x) = \{Re(A) = Im(B) = 0\}$. $p_\pm$ is a sink within $P_\pm$.

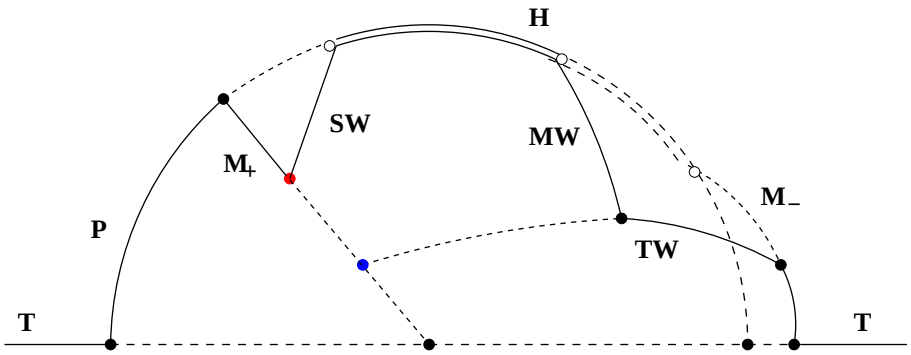

Figure 16: Bifurcation diagram along a path encircling $\mu_1 = \mu_2 = 0$ closely, showing local and global bifurcations (filled and open dots respectively). Solid and dashed lines indicate stable and unstable solutions. T - trivial solution $A = B = 0$; H - heteroclinic cycle, other solution labels are defined in the text.

where λ_c and λ_e are the relevant ('contracting' and 'expanding') eigenvalues at $p_\pm$. This yields $\mu_1 - b_1\mu_2/a_2 < 0$ which is the straight dash-dotted line *delta=1* in figure 13. When $\delta = 1$ we have a resonant bifurcation of the cycle and the cycle loses asymptotic stability. A stable long period periodic orbit appears near the cycle: this is the modulated wave (MW) solution indicated on figure 13. The MW solution is destroyed at a Hopf bifurcation with the TW solutions, as indicated in figure 16 which summarises the bifurcation sequence following a small circle around the origin $\mu_1 = \mu_2 = 0$.

4.3 The Guckenheimer–Holmes cycle

Along with the cycle in the $1:2$ mode interaction discussed in the previous section, the Guckenheimer–Holmes (GH) cycle has become one of the standard examples in the literature. In fact the literature goes back further than the GH paper [29], in at least two directions. One is that of fluid mechanics; the other is mathematical ecology. In the fluid mechanics context, Küppers & Lortz [39] performed a linear stability analysis of convection rolls in a rotating fluid layer, under various assumptions (infinite domain size, Boussinesq fluid, small Froude number, infinite Prandtl number). For small nondimensionalised rotation rates (values of a Taylor number Ta) straight rolls are linearly stable. For larger Ta they become unstable, with the instability occuring first to rolls aligned at approxi-

mately 58° to the original ones. This paper was followed later by various weakly nonlinear analyses by Busse and co-workers [12; 6] and by Soward [52]. Guckenheimer & Holmes [29] provided proofs that the dynamics of the weakly nonlinear ODEs that had been proposed were indeed as previous authors had described. In the mathematical ecology literature, the same ODEs had in fact been written down by May & Leonard [40]. We will not dwell on any physical or biological interpretation here: the mathematical description will be enough to discuss various general questions that arise in the study of robust cycles.

Consider the absolutely irreducible representation of $\mathbb{Z}_3 \ltimes \mathbb{Z}_2^3$ on $\mathbb{R}^3$ generated by

$$\begin{aligned} \sigma(x_1, x_2, x_3) &= (x_2, x_3, x_1), \\ \kappa_1(x_1, x_2, x_3) &= (-x_1, x_2, x_3). \end{aligned}$$

We define κ_2 and κ_3 by analogy. This symmetry group arises in the pattern formation context of hexagonal planforms in a rotating fluid layer. The rotation reduces the overall physical symmetry from $E(2)$ to the special Euclidean group $SE(2)$ of translations and rotations (but no reflections) of the fluid layer. There are exactly two (group orbits of) axial isotropy subgroups:

$$\Sigma_1 = \{I, \kappa_2, \kappa_3, \kappa_2\kappa_3\} \qquad \mathrm{Fix}(\Sigma_1) = (x, 0, 0) \tag{42}$$

$$\Sigma_2 = \{I, \sigma, \sigma^2\} \qquad \mathrm{Fix}(\Sigma_2) = (x, x, x) \tag{43}$$

In phase space, the symmetries κ_j, which are derived from translation symmetries in physical space, act as reflections and make the hyperplanes $x_j = 0$ (and all subspaces that are intersections of these planes) invariant for the dynamics. Since (42) - (43) define axial isotropy subgroups there are guaranteed solution branches by the EBL. Equivariant amplitude equations (truncated at cubic order) take the form

$$\dot{x}_1 = x_1[\mu + ax_1^2 + bx_2^2 + cx_3^2], \tag{44}$$

$$\dot{x}_2 = x_2[\mu + ax_2^2 + bx_3^2 + cx_1^2], \tag{45}$$

$$\dot{x}_3 = x_3[\mu + ax_3^2 + bx_1^2 + cx_2^2]. \tag{46}$$

Interestingly, for some combinations of the real coefficients a, b, c there exist 'bimodal' equilibria with submaximal isotropy, for example

$$x_1^2 = \frac{\mu(b-a)}{a^2 - bc}, \quad x_2^2 = \frac{\mu(c-a)}{a^2 - bc}, \quad x_3 = 0,$$

which only exist if $c - a$ and $b - a$ have the same sign. For fixed $\mu > 0$ and $a^2 - bc > 0$, consider what happens as one of $c - a$ and $b - a$ goes through zero. We observe a local pitchfork bifurcation of the axis equilibria as the 'bimodal' equilbria disappear. This change is sketched in figure 17. For

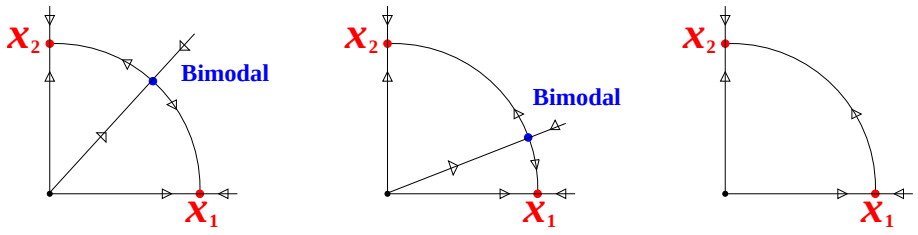

Figure 17: Possible dynamics in the (x_1, x_2) invariant plane for $\mu > 0$ and $a < 0$. (a), (b) bimodal equilibria exist in the interior of the invariant plane. (c) no bimodal equilibria exist when $b < a < c$: instead there is a robust connection between $(x, 0, 0)$ and $(0, x, 0)$.

an open set of coefficient values, the equilibrium $(0, x, 0)$ is a sink within $\mathrm{Fix}(\kappa_3) = (x_1, x_2, 0)$ and

there is a robust saddle-sink connecting orbit as in figure 17(c). By symmetry there are similar connecting orbits in the other coordinate hyperplanes, leading to the formation of the cycle, see figure 18. So, now keeping a, b and c fixed and varying μ through zero we have a steady-state

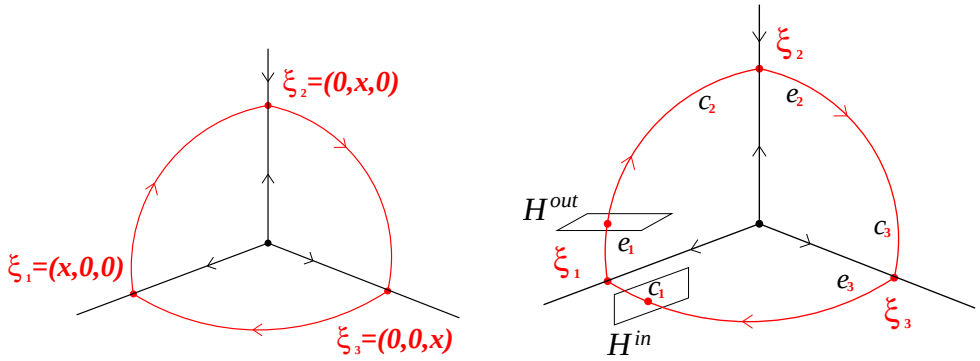

Figure 18: (a) The $\mathbb{Z}_3 \ltimes \mathbb{Z}_2^3$-symmetric May–Leonard–Busse–Heikes–Guckheimer–Holmes robust homoclinic cycle. (b) A $\mathbb{Z}_2^3$-equivariant flow containing a robust heteroclinic cycle in $\mathbb{R}^3$. c_j and e_j are the eigenvalues of the linearisation at the equilibrium ξ_j, in the 'incoming' (contracting) and 'outgoing' (expanding) directions.

bifurcation that results in heteroclinic cycling rather than in a new stable equilibrium state. It turns out that more complicated scenarios are possible: steady-state bifurcations can give rise to branches of periodic orbits (Field & Swift [21]) or indeed chaotic attractors (called 'instant chaos' by Guckenheimer & Worfolk [30]) directly at the bifurcation point.

Stability for the GH cycle in $\mathbb{R}^3$

To compute stability of a heteroclinic cycle, the standard approach is to construct Poincaré return maps using the linearised flow near each equilibrium to construct local and global maps for trajectories near the cycle. The local map $\phi : H_1^{in} \to H_1^{out}$, where $H_1^{in} = \{x_2 = h\}$ and $H_1^{out} = \{x_3 = h\}$, is illustrated in figure 18(b). The global map $\psi : H_1^{out} \to H_3^{in}$ is a diffeomorphism that respects the symmetry of the flow. Such a construction enables a proper statement of the set of initial conditions whose trajectories converge to, or diverge from, a neighbourhood of the cycle. Hofbauer and Sigmund [31] use an equivalent method based on defining 'average Liapounov functions' to investigate the behaviour of trajectories near the cycle.

A quick-and-dirty method applicable to the cycles sketched in figure 18 is to use the linearised flow to estimate the times spent within a neighbourhood of each equilibrium. If this sequence of times increases then the trajectory must be converging to the cycle. Working with figure 18(b), suppose that a trajectory crosses H_3^{in} and exits at H_2^{out} after spending times $T_n(\xi_3)$ near ξ_3 and $T_n(\xi_2)$ near ξ_2. Then

$$h\exp(-c_3T_n(\xi_3) + e_2T_n(\xi_2)) = h, \qquad \Rightarrow T_n(\xi_2) = \frac{c_3}{e_2}T_n(\xi_3),$$

where c_j and e_j are the eigenvalues of the linearisation at the equilibrium ξ_j, in the 'incoming' (contracting) and 'outgoing' (expanding) directions. Similarly we find that $T_n(\xi_1) = \frac{c_2}{e_1}T_n(\xi_2)$ and, considering the trajectory passing through neighbourhoods of ξ_1 and ξ_3 for a second time, $T_{n+1}(\xi_3) = \frac{c_1}{e_3}T_n(\xi_1)$. Putting all this together we obtain

$$T_{n+1}(\xi_3)/T_n(\xi_3) \quad = \quad \frac{c_1c_2c_3}{e_1e_2e_3}$$

and so the length of time spent near each equilibrium increases if $\prod c_j > \prod e_j$. When this inequality becomes an equality a resonant bifurcation occurs, and trajectories move away from the cycle. As

we saw in section 4.2 for the 1 : 2 mode interaction case, resonant bifurcations typically generate long period periodic orbits lying close to the cycle. In section 4.2 the modulated wave (MW) orbit appeared at the line $\delta = 1$. In the present case, for (44) - (46), the resonant bifurcation occurs when $2a = b + c$, but for the amplitude equations truncated at cubic order the bifurcation is degenerate since the equations have a conserved quantity when $2a = b + c$ and the equilibrium at (x, x, x) is a centre.

To produce a better model of reality it is of interest to consider disturbing the idealised ODEs (44) - (46) by breaking the symmetries slightly, or adding noise perturbations. In these cases we find that the heteroclinic cycling turns into approximately periodic oscillations between neighbourhoods of the three equilibria. In the noisy case, the period of the oscillations $T \sim \log(1/\varepsilon)$ where ε is a measure of the noise amplitude.

4.4 Stability results and bifurcations

In this section we will first state a very general result giving sufficient conditions for stability of heteroclinic cycles in $\mathbb{R}^n$ due to Krupa & Melbourne [37]. We will then specialise to $\mathbb{R}^4$ and discuss three particular examples.

For robust *homoclinic* cycles in $\mathbb{R}^4$ there is a complete classification of the different types due to Sottocornola [50; 51], applying the necessary and sufficient conditions on the group action developed by Ashwin & Montaldi [2]. For heteroclinic cycles there are various results concerning stability and bifurcations, but in higher dimensions the situation is less clear and little is in general known. Intuitively, a cycle should be stable if the 'contracting' eigenvalue in the direction a trajectory approaches each equilibrium is larger in magnitude than the 'expanding' one in the direction it follows on leaving, but some subtleties appear due to the existence of more directions ('transverse' to the cycle). Of necessity we must first introduce some definitions for 'expanding' and 'contracting' to make this more precise.

Let $\xi_1, \ldots, \xi_k$ be a sequence of equilibria for the ODEs $\dot{x} = f(x)$ which form a heteroclinic cycle. We assume

Hypotheses (H).

- ξ_j is a hyperbolic equilibrium point for all j
- the unstable manifold $W^u(\xi_j) \setminus \{\xi_j\}$ lies entirely within a fixed point subspace $P_j = \mathrm{Fix}(\Sigma_j)$ for some isotropy subgroup Σ_j.

Let T_j be the isotropy subgroup of the equilibrium ξ_j. We define the subspace $L_j = \mathrm{Fix}(T_j)$. Then $\mathbb{R}^n$ can be isotypically decomposed with respect to the action of T_j into four isotypic components:

$$\mathbb{R}^n \quad = \quad L_j \oplus V_j(c) \oplus V_j(e) \oplus V_j(t) \tag{47}$$

using the fact that T_j acts trivially on L_j but non-trivially and differently on all the other spaces since $\Sigma_{j-1} \neq \Sigma_j$, $\Sigma_j \subset T_j$ and so $V_j(e)$ is the complement to L_j in P_j. Similarly $\Sigma_{j-1} \subset T_j$ so $V_j(c)$ is the complement to L_j in P_{j-1}. Then for each subspace we can select the largest of the eigenvalues of the Jacobian $Df(\xi_j)$ restricted to that subspace, see table 7. Although the notation L_j and P_j is suggestive of lines and planes, we leave open, at this stage, the possibilities that dim $L_j > 1$ or dim $P_j > 2$. Then we can state the general result of Krupa & Melbourne.

Theorem 13 (Krupa & Melbourne [37]) *Assuming hypotheses (H), the heteroclinic cycle X is asymptotically stable if*

$$t_j < 0 \qquad \text{and} \qquad \prod_{j=1}^{k} \min(c_j, e_j - t_j) \quad > \quad \prod_{j=1}^{k} e_j. \tag{48}$$

	Eigenvalues of $Df(\xi_j)$	Subspace
radial	$-r_j = \max_{\lambda \in \mathrm{spec}(Df(\xi_j)^r)} \mathrm{Re}(\lambda)$	$L_j \equiv P_{j-1} \cap P_j$
contracting	$-c_j = \max_{\lambda \in \mathrm{spec}(Df(\xi_j)^c)} \mathrm{Re}(\lambda))$	$P_{j-1} \setminus L_j$
expanding	$e_j = \max_{\lambda \in \mathrm{spec}(Df(\xi_j)^e)} \mathrm{Re}(\lambda))$	$P_j \setminus L_j$
transverse	$t_j = \max_{\lambda \in \mathrm{spec}(Df(\xi_j)^t)} \mathrm{Re}(\lambda))$	$(P_{j-1} + P_j)^\perp$

Table 7: Definitions of the four eigenvalue classes: $-c_j < 0$ contracting; $e_j > 0$ expanding; $-r_j < 0$ radial; t_j transverse. $\mathrm{spec}(Df(\xi_j)^{r,c,e,t})$ denotes the spectrum of $Df(\xi_j)$ restricted to the subspaces L_j, $V_j(c)$, $V_j(e)$, $V_j(t)$ respectively. $P_j \setminus L_j$ denotes the orthogonal complement in P_j of the subspace L_j, see figure 19.

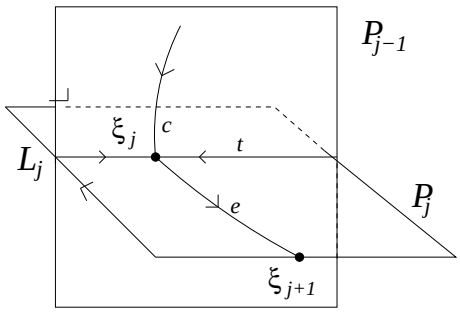

Figure 19: Sketch of the subspaces P_{j-1}, P_j and L_j near equilibria ξ_j and ξ_{j+1}.

Krupa & Melbourne [37] proved that these sufficient conditions were in fact also necessary, as long as two further hypotheses are satisfied:

Hypotheses (H').

- the eigenspaces corresponding to c_j, t_j, e_{j+1} and t_{j+1} lie in the same Σ_j-isotypic component.
- $\dim W^u(\xi_j) = 1$,

Note that the first of these conditions refers to a different isotypic decomposition to that with respect to T_j in (47). Hypotheses (H) and (H') are satisfied for both examples discussed previously; the $1:2$ mode interaction problem and the Guckenheimer–Holmes cycle. In fact, all cycles in $\mathbb{R}^3$ satisfy (H') because $\dim \mathrm{Fix}(\Sigma_j) = 2$ and so c_j and e_{j+1} are the same direction (there can be no transverse eigenvalues). For a homoclinic cycle in $\mathbb{R}^3$ the condition for asymptotic stability is just $\delta \equiv c/e > 1$.

The existence of transverse directions introduces a subtlety into the notion of stability of a heteroclinic cycle. Cycles with positive transverse eigenvalues (and so both the second part of hypothesis (H) and the inequality (48) are not satisfied) may still be strongly attracting, in the sense of being *essentially asymptotically stable* [42].

An invariant set X is essentially asymptotically stable (e.a.s.) if there exists a set $\mathcal{A}$ such that given any real number $a \in (0,1)$, and any neighbourhood $\mathcal{U}$ of X, there is an open neighbourhood $\mathcal{V} \subset \mathcal{U}$ of X such that:

1. All trajectories starting in $\mathcal{V} \setminus \mathcal{A}$ remain in $\mathcal{U}$,
2. All trajectories starting in $\mathcal{V} \setminus \mathcal{A}$ are asymptotic to X,
3. $\mu(\mathcal{V} \setminus \mathcal{A})/\mu(\mathcal{V}) > a$, where μ is Lebesgue measure.

This means that initial conditions in an arbitrarily large proportion of a neighbourhood are attracted to X, if we look at smaller and smaller neighbourhoods of X.

Simple cycles in $\mathbb{R}^4$

We now turn to a much more specific situation, that of simple cycles in $\mathbb{R}^4$. Homoclinic cycles are discussed in detail by Chossat et al. [8]: heteroclinic cycles are discussed by Krupa & Melbourne [38]. The specific examples we discuss here are homoclinic cycles for simplicity. The robust cycle $X \subset \mathbb{R}^4 \setminus \{0\}$ is simple if

- $\dim P_j = 2$ for all j,
- X intersects each connected component of $L_j \setminus \{0\}$ in at most one point.

Then the second part of hypothesis (H') is always satisfied, and there is precisely one eigenvalue of each type r, c, e, t. The first part of (H') may or may not be satisfied; this leads to conditions for stability that improve on (48). Define the three-dimensional subspace $Q = P_1 + P_k$ (focusing on ξ_1 since all equilibria lie on a single group orbit in the homoclinic case). Then homoclinic cycles in $\mathbb{R}^4$ can be classified into one of three types:

- X is of type A if Q is not a fixed point subspace,
- X is of type B if Q is a fixed point subspace and $X \subset Q$,
- X is of type C if Q is a fixed point subspace but $X \not\subset Q$.

To give a flavour of these possibilities we describe examples of each, and the typical behaviour when each undergoes a transverse bifurcation.

Type A. In this case it follows that (H') is satisfied and condition (48) is necessary and sufficient for stability. Consider the action of the group $\mathcal{T}$ generated by the two elements

$$\sigma = \begin{pmatrix} 0 & 1 & 0 & 0 \\ 0 & 0 & 1 & 0 \\ 1 & 0 & 0 & 0 \\ 0 & 0 & 0 & 1 \end{pmatrix} \quad \text{and} \quad \kappa = \begin{pmatrix} -1 & 0 & 0 & 0 \\ 0 & 1 & 0 & 0 \\ 0 & 0 & 1 & 0 \\ 0 & 0 & 0 & -1 \end{pmatrix}$$

(see [10], example 9.2.12, and [9]). At cubic order the equivariant amplitude equations are

$$\dot{x}_1 = \mu_1 x_1 + x_1(a_1 x_1^2 + a_2 x_2^2 + a_3 x_3^2) + a_4 x_2 x_3 x_4 \tag{49}$$
$$\dot{x}_2 = \mu_1 x_2 + x_2(a_1 x_2^2 + a_2 x_3^2 + a_3 x_1^2) + a_4 x_1 x_3 x_4 \tag{50}$$
$$\dot{x}_3 = \mu_1 x_3 + x_3(a_1 x_3^2 + a_2 x_1^2 + a_3 x_2^2) + a_4 x_1 x_2 x_4 \tag{51}$$
$$\dot{x}_4 = \mu_2 x_4 + b_1 x_4^3 + b_2 x_1 x_2 x_3 \tag{52}$$

It can be checked that, as in the Guckenheimer–Holmes example, when $a_2 < a_1 < a_3 < 0$ there is a homoclinic cycle for $\mu_1 > 0$, between the symmetry-related equilibria $(x_1, 0, 0, 0)$, $(0, x_2, 0, 0)$ and $(0, 0, x_3, 0)$. The planes $(x_1, x_2, 0, 0)$, $(0, x_2, x_3, 0)$ and $(x_1, 0, x_3, 0)$ are fixed point subspaces for a single reflection symmetry and hence have isotropy subgroups isomorphic to $\mathbb{Z}_2$. Since the only subgroup of $\mathbb{Z}_2$ is $\{I\}$ there are no three-dimensional fixed point subspaces (alternatively, by inspection of the form of the amplitude equations). So this cycle is of type A. Setting $\mu_1 = 1$ for simplicity we find the eigenvalues at the equilibrium $\xi_1 = (\sqrt{-1/a_1}, 0, 0, 0)$ to be

$$-r = -2, \qquad -c = 1 - a_2/a_1, \qquad e = 1 - a_3/a_1, \qquad t = \mu_2.$$

Hence the cycle is stable when $\mu_2 < 0$ and $a_2 - a_1 < a_1 - a_3$.

Resonant bifurcations from a type A cycle give rise to long-period periodic orbits, but of two slightly different kinds depending on whether the periodic orbit twists on its way from one equilibrium to the next, or not ([10], p345).

Transverse bifurcations from type A cycles have similar properties to resonant ones, giving rise to long-period orbits that remain exponentially close the the cycle ($O(\Delta^{1/\mu})$ where μ is the bifurcation parameter and $\Delta \neq 1$ is a constant). An example with ODEs similar to (49) - (52) occurs in oscillatory pattern formation in a rotating fluid layer, see Dawes[14].

Type B. In this case (H') fails but necessary and sufficient conditions for stability are still given by (48). A simple example of a type B cycle is given by embedding the Guckenheimer–Holmes cycle in $\mathbb{R}^3$ into a subspace $x_4 = 0$ of $\mathbb{R}^4$. For example, consider the group $\mathbb{Z}_3 \ltimes \mathbb{Z}_2^3 \times \mathbb{Z}_2$ generated by

$$\sigma = \begin{pmatrix} 0 & 1 & 0 & 0 \\ 0 & 0 & 1 & 0 \\ 1 & 0 & 0 & 0 \\ 0 & 0 & 0 & 1 \end{pmatrix} \qquad \kappa_1 = \begin{pmatrix} -1 & 0 & 0 & 0 \\ 0 & 1 & 0 & 0 \\ 0 & 0 & 1 & 0 \\ 0 & 0 & 0 & 1 \end{pmatrix} \quad \text{and} \quad \kappa_4 = \begin{pmatrix} 1 & 0 & 0 & 0 \\ 0 & 1 & 0 & 0 \\ 0 & 0 & 1 & 0 \\ 0 & 0 & 0 & -1 \end{pmatrix}$$

where σ and κ_1 act on $\mathbb{R}^3$ just as in section 4.3 and κ_4 generates the new $\mathbb{Z}_2$ part of the group. The three-dimensional subspace $Q = P_1 + P_3 = (x_1, x_2, x_3, 0) \supset X$ is clearly $\mathrm{Fix}(\kappa_4)$ so it is a fixed point space containing the cycle X. A possible set of amplitude equations, truncated at cubic order again is

$$\begin{aligned} \dot{x}_1 &= \mu_1 x_1 + x_1(a_1 x_1^2 + a_2 x_2^2 + a_3 x_3^2 + a_4 x_4^2) && (53) \\ \dot{x}_2 &= \mu_1 x_2 + x_2(a_1 x_2^2 + a_2 x_3^2 + a_3 x_1^2 + a_4 x_4^2) && (54) \\ \dot{x}_3 &= \mu_1 x_3 + x_3(a_1 x_3^2 + a_2 x_1^2 + a_3 x_2^2 + a_4 x_4^2) && (55) \\ \dot{x}_4 &= \mu_2 x_4 + b_1 x_4^3 + b_2 x_4(x_1^2 + x_2^2 + x_3^2) && (56) \end{aligned}$$

As in the type A case, a transverse bifurcation occurs when μ_2 passes through zero. This pitchfork bifurcation at each equilibrium ξ_j on the cycle generically produces a pair of new equilibria $\xi_j^{\pm}$. The transverse bifurcation results in two new heteroclinic cycles, one connecting all the ξ_j^+ equilibria and one connecting all the ξ_j^- equilibria. This is sketched in figure 20; these sketches make use of the Invariant Sphere Theorem [20]:

Theorem 14 (The Invariant Sphere Theorem) *Let $\dot{x} = \mu x + Q(x)$ be a collection of $\mathcal{G}$-equivariant ODEs in $\mathbb{R}^n$ such that*

- *$Q(x)$ contains only polynomial terms of cubic order in $x_1, \ldots, x_n$,*
- *$Q(x) \cdot x < 0$ for all $x \neq 0$ (Q is then said to be contracting).*

Then for every $\mu > 0$ there exists a unique flow-invariant topological $n-1$–sphere $S_\mu \subset \mathbb{R}^n \setminus \{0\}$ which is globally attracting.

The Invariant Sphere theorem enables us to sketch the dynamics of the four-dimensional examples of type B and C cycles, by sketching a tetrahedron corresponding to the intersection of the positive quadrant $\mathbb{R}^4_+$ with the invariant 3-sphere. In the three dimensional Guckenheimer–Holmes case we would need only to sketch the triangle formed by the projections of the three connecting orbits onto a 2-sphere.

Figure 20(a) illustrates the dynamics of (53) - (56) in the case $\mu_2 > 0$, $b_1 < 0$ when the transverse bifurcation has created stable equilibria that lie on the edges 14, 24 and 34. By considering the dynamics within the (flow-invariant) faces 124, 234 and 134 we can establish the existence of a robust heteroclinic cycle between these three new equilibria. Hence in a transverse bifurcation from a type B cycle we generate new global dynamics as well as new local equilibria.

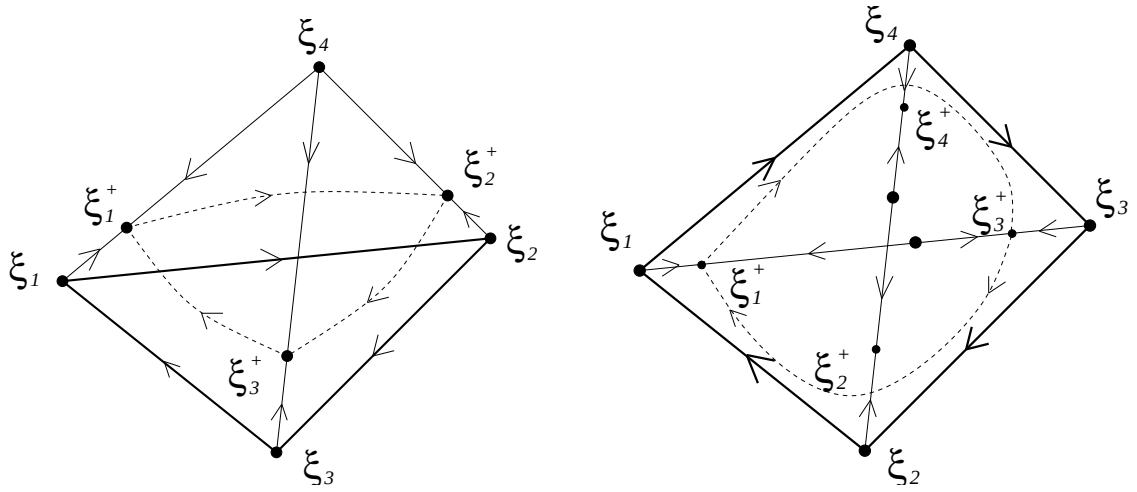

Figure 20: Tetrahedrons within the invariant 3-sphere showing original heteroclinic 'edge' cycles (bold lines) and bifurcating 'face' cycles (dashed lines). (a) Type B cycle: $\xi_1^+ \to \xi_2^+ \to \xi_3^+ \to \xi_1^+$. (b) Type C cycle: $\xi_1^+ \to \xi_3^+ \to \xi_1^+$. A symmetrically-related cycle $\xi_2^+ \to \xi_4^+ \to \xi_2^+$ also exists but the connecting orbits are not shown here.

Type C. In this case (H') fails again, and necessary and sufficient conditions for asymptotic stability are

$$c - t > e \qquad \text{and} \qquad t < 0. \tag{57}$$

A well known example of a type C cycle is that of Field & Swift [21]. Consider the group $\mathbb{Z}_4 \ltimes \mathbb{Z}_2^4$ acting on $\mathbb{R}^4$ and generated by

$$\sigma = \begin{pmatrix} 0 & 1 & 0 & 0 \\ 0 & 0 & 1 & 0 \\ 0 & 0 & 0 & 1 \\ 1 & 0 & 0 & 0 \end{pmatrix} \qquad \text{and} \qquad \kappa_1 = \begin{pmatrix} -1 & 0 & 0 & 0 \\ 0 & 1 & 0 & 0 \\ 0 & 0 & 1 & 0 \\ 0 & 0 & 0 & 1 \end{pmatrix}$$

This group action is absolutely irreducible, and gives rise to the amplitude equations

$$\begin{aligned} \dot{x}_1 &= \mu x_1 + a_1 x_1 X^2 + x_1(a_2 x_2^2 + a_3 x_3^2 + a_4 x_4^2) \\ \dot{x}_2 &= \mu x_2 + a_1 x_2 X^2 + x_2(a_2 x_3^2 + a_3 x_4^2 + a_4 x_1^2) \\ \dot{x}_3 &= \mu x_3 + a_1 x_3 X^2 + x_3(a_2 x_4^2 + a_3 x_1^2 + a_4 x_2^2) \\ \dot{x}_4 &= \mu x_4 + a_1 x_4 X^2 + x_4(a_2 x_1^2 + a_3 x_2^2 + a_4 x_3^2) \end{aligned}$$

where $X^2 = x_1^2 + x_2^2 + x_3^2 + x_4^2$. By taking a_1 sufficiently negative we can ensure that the conditions for the Invariant Sphere Theorem to hold are satisfied and all branches of equilibria bifurcate supercritically. When in addition $a_2 a_4 < 0$ there are two edge equilibria, and a heteroclinic cycle exists between the four equilibria lying on the axes (corresponding to the vertices in the tetrahedron in figure 20(b)). To check that this cycle is of type C we consider the union of the subspaces containing the 43 and the 32 connections: this is $Q = P_4 + P_3 = (0, x_2, x_3, x_4)$. But $Q = \mathrm{Fix}(\kappa_1)$ so Q is a fixed point subspace that does not contain the entire cycle X. Field & Swift prove that the cycle is stable if and only if $a_3 < 0$ and $a_2 + a_3 + a_4 < 0$ which are the conditions given in (57).

4.5 Heteroclinic networks

If a system contains more than one heteroclinic cycle they may be coupled together to form a heteroclinic network. Ashwin and Field (1999) provide a very general definition of a heteroclinic network;

in these notes we will only be concerned with flows in $\mathbb{R}^n$ where each node in the network is an equilibrium of the flow (rather than e.g. a periodic orbit, a chaotic set or, indeed, another heteroclinic cycle). For the example below, the following definition is sufficient. An invariant set N consisting of equilibria $\{\xi_1, ..., \xi_n\}$ and heteroclinic orbits $\{\gamma_1, ..., \gamma_m\}$ is a (depth 1) robust heteroclinic network if

1. (compatibility) if $x \in \gamma_i$ then $\alpha(x) = \xi_j$ and $\omega(x) = \xi_k$ for some $\xi_j, \xi_k \in N$.
2. (transitivity) for all ξ_i and ξ_j we can find a sequence of orbits $\{\gamma_{m_1}, ..., \gamma_{m_l}\}$ and equilibria $\{\xi_{n_1}, ..., \xi_{n_{l+1}}\}$ such that $\xi_{n_1} = \xi_i$ and $\xi_{n_{l+1}} = \xi_j$ and if $x \in \gamma_{m_k}$ then $\alpha(x) = \xi_{n_k}$ and $\omega(x) = \xi_{n_{k+1}}$.
3. (robustness) any compatible set of equilibria $\xi_1, \ldots, \xi_n$, $\xi_{n+1} \equiv \xi_1$, and connecting orbits $\xi_i \to \xi_{i+1}$, forms a robust heteroclinic cycle.

where $\alpha(x)$ and $\omega(x)$ are the usual limit sets. Transitivity means that if we draw the network as a directed graph between equilibria, then a path exists between any two equilibria in the network.

Heteroclinic networks contain many heteroclinic 'sub-cycles'. Unless the network has only one cycle (i.e it is itself a heteroclinic cycle) then none of these sub-cycles can be asymptotically stable, because each sub-cycle must contain at least one equilibrium with a two-dimensional unstable manifold, (by the transitivity property) so there will be points near the cycle which are contained in a heteroclinic orbit to an equilibrium not contained in the cycle. However, sub-cycles can still be essentially asymptotically stable.

If condition 3 in the definition of essential asymptotic stability is relaxed to $\mu(\mathcal{V} \setminus \mathcal{A}) > 0$ then the set X is an attractor in a weaker sense and is called a Milnor attractor [43]; any set which is e.a.s. is also a Milnor attractor.

A simple example of a heteroclinic network in $\mathbb{R}^4$ with two sub-cycles was studied by Kirk and Silber [34] (and Brannath [4]). They found that it was not possible for both sub-cycles to be simultaneously e.a.s., however they could both be attracting in some sense, and the network considered as a whole could be e.a.s.. Kirk and Silber also found that if one sub-cycle is unstable, then 'switching' between the sub-cycles could occur. That is, a trajectory starting close to the network may make a number of excursions near to one of the cycles, and then switch to cycling near the other. With only two sub-cycles in their example, the switching could only occur in one direction, so there are no initial conditions near the cycle that have ω-limit sets equal to the entire network.

In the rest of this section we will outline the numerical results of Postlethwaite & Dawes [46] who observed irregular switching of trajectories near a heteroclinic network in $\mathbb{R}^6$. Little is known about the behaviour near heteroclinic networks in general, and this kind of behaviour may be typical of higher-dimensional problems.

Regular and irregular cycling sub-cycles

Postlethwaite & Dawes [46] consider $\mathbb{Z}_6 \ltimes \mathbb{Z}_2^6$-symmetric ODEs in $\mathbb{R}^6$, with a cubic truncation

$$\dot{x}_1 = x_1(1 - X^2 + ex_2^2 - cx_3^2 - s_3y_1^2 + s_2y_2^2 - s_1y_3^2) \quad (58)$$
$$\dot{x}_2 = x_2(1 - X^2 + ex_3^2 - cx_1^2 - s_3y_2^2 + s_2y_3^2 - s_1y_1^2) \quad (59)$$
$$\dot{x}_3 = x_3(1 - X^2 + ex_1^2 - cx_2^2 - s_3y_3^2 + s_2y_1^2 - s_1y_2^2) \quad (60)$$
$$\dot{y}_1 = y_1(1 - X^2 + ey_2^2 - cy_3^2 - s_3x_1^2 + s_2x_2^2 - s_1x_3^2) \quad (61)$$
$$\dot{y}_2 = y_2(1 - X^2 + ey_3^2 - cy_1^2 - s_3x_2^2 + s_2x_3^2 - s_1x_1^2) \quad (62)$$
$$\dot{y}_3 = y_3(1 - X^2 + ey_1^2 - cy_2^2 - s_3x_3^2 + s_2x_1^2 - s_1x_2^2) \quad (63)$$

where $X^2 = \sum_{i=1}^3 (x_i^2 + y_i^2)$. These ODEs can be thought of as two Guckenheimer-Holmes cycles in the subspaces $(x_1, x_2, x_3, 0, 0, 0)$ and $(0, 0, 0, y_1, y_2, y_3)$ with the possibility of more heteroclinic

orbits connecting equilibria in each cycle together. For the Guckenheimer–Holmes cycles, e and c are the expanding and contracting eigenvalues, and there are three transverse eigenvalues s_1, s_2, s_3.

Consider the case where $s_j > 0$, $j = 1, 2, 3$. Then the network of connecting orbits between equilibria on the axes is as given in figure 21. In this figure the equilibria $\xi_1 = (x_1, 0, 0, 0, 0, 0)$ and

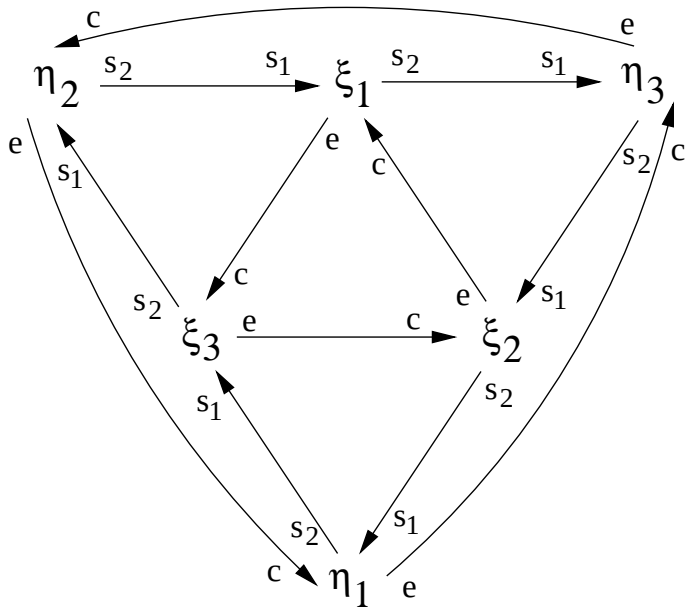

Figure 21: Sketch of the network of connecting orbits between equilibria ξ_1, ξ_2, ξ_3 and η_1, η_2, η_3. The ξ_j equilibria and η_j equilibria separately form Guckenheimer–Holmes cycles.

$\eta_1 = (0, 0, 0, y_1, 0, 0)$; $\xi_2, \xi_3, \eta_2, \eta_3$ are defined similarly. The network of connections clearly contains many other heteroclinic sub-cycles, for example $\xi_2 \to \xi_1 \to \eta_3 \to \xi_2$ and $\eta_3 \to \eta_2 \to \xi_1 \to \eta_3$ and symmetric copies of these. None of these sub-cycles can be asymptotically stable since each equilibrium has a two dimensional unstable manifold. For an open region of choices of the coefficients in the amplitude equations (58) - (63) we observe 'cycling sub-cycles' behaviour, illustrated by a time series plot in figure 22, and schematically in figure 23. Both figures show a trajectory switching from a neighbourhood of the $\xi_2 - \xi_1 - \eta_3$ cycle to a neighbourhood of the $\eta_1 - \eta_3 - \xi_2$ cycle and then to the $\xi_3 - \xi_2 - \eta_1$ cycle. For some combinations of coefficients trajectories settle down to performing a constant number of loops n around each sub-cycle. For a single set of coefficients, varying the initial conditions can give rise to stable looping with many different values of n. Postlethwaite & Dawes call this 'regular cycling'. For other combinations of coefficients, no stable regular cycling is possible and trajectories perform a bounded but aperiodic sequence of numbers of loops around each sub-cycle. This is the 'irregular cycling' case. The 'regular' and 'irregular' cases are illustrated in figure 24.

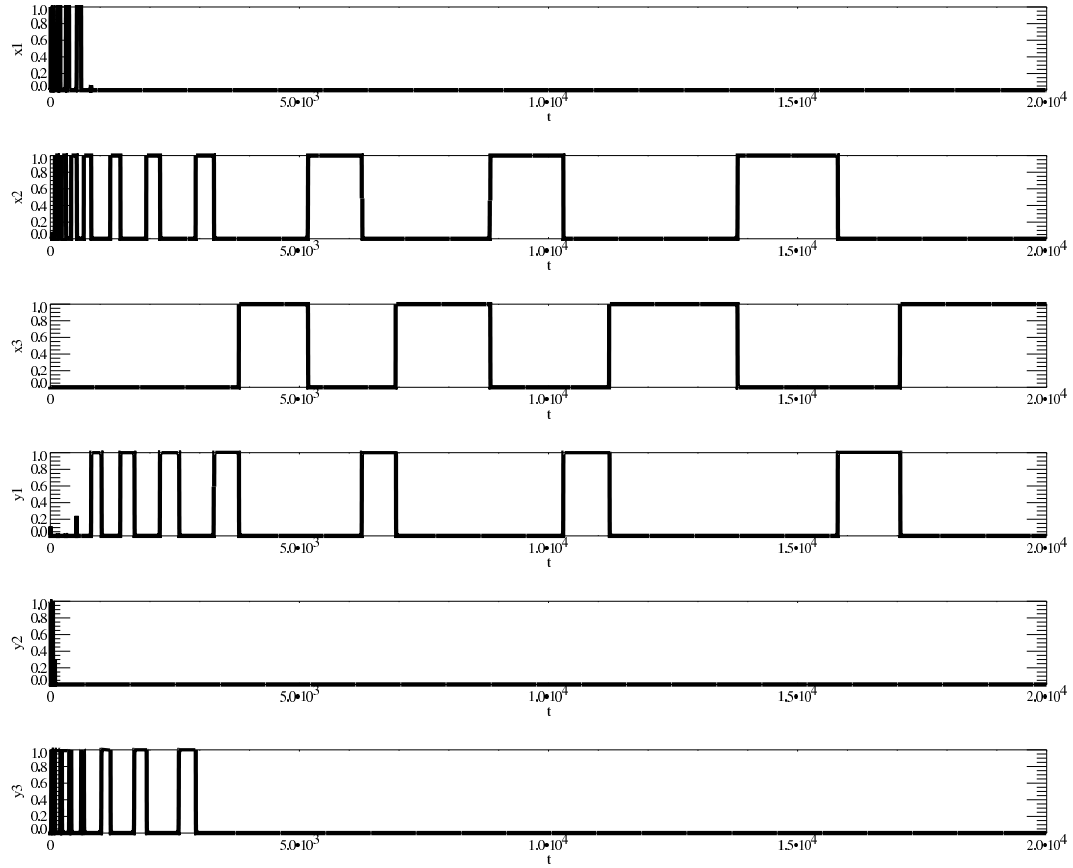

Figure 22: Time integration of (58) - (63), showing cycling sub-cycles. Coordinates $x_1, \ldots, y_3$ are plotted, top to bottom. The cycles are visited in the order $\xi_2 - \xi_1 - \eta_3$; $\eta_1 - \eta_3 - \xi_2$; $\xi_3 - \xi_2 - \eta_1$. Parameter values are $c = 1.0$, $e = 0.5$, $s_1 = 1.4$, $s_2 = 1.6$, $s_3 = 1.1$, $t_1 = 0.9$, $t_2 = 0.7$, $t_3 = 0.9$.

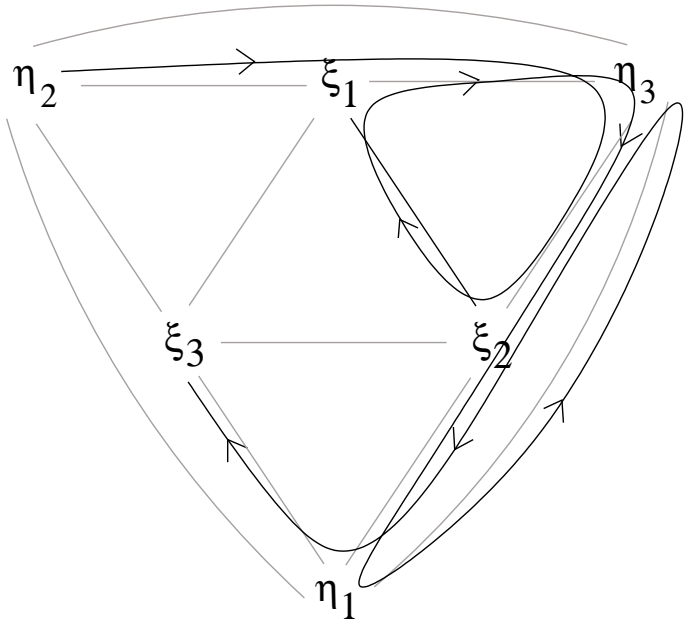

Figure 23: Schematic diagram of a cycling sub-cycles trajectory; compare with figure 22.

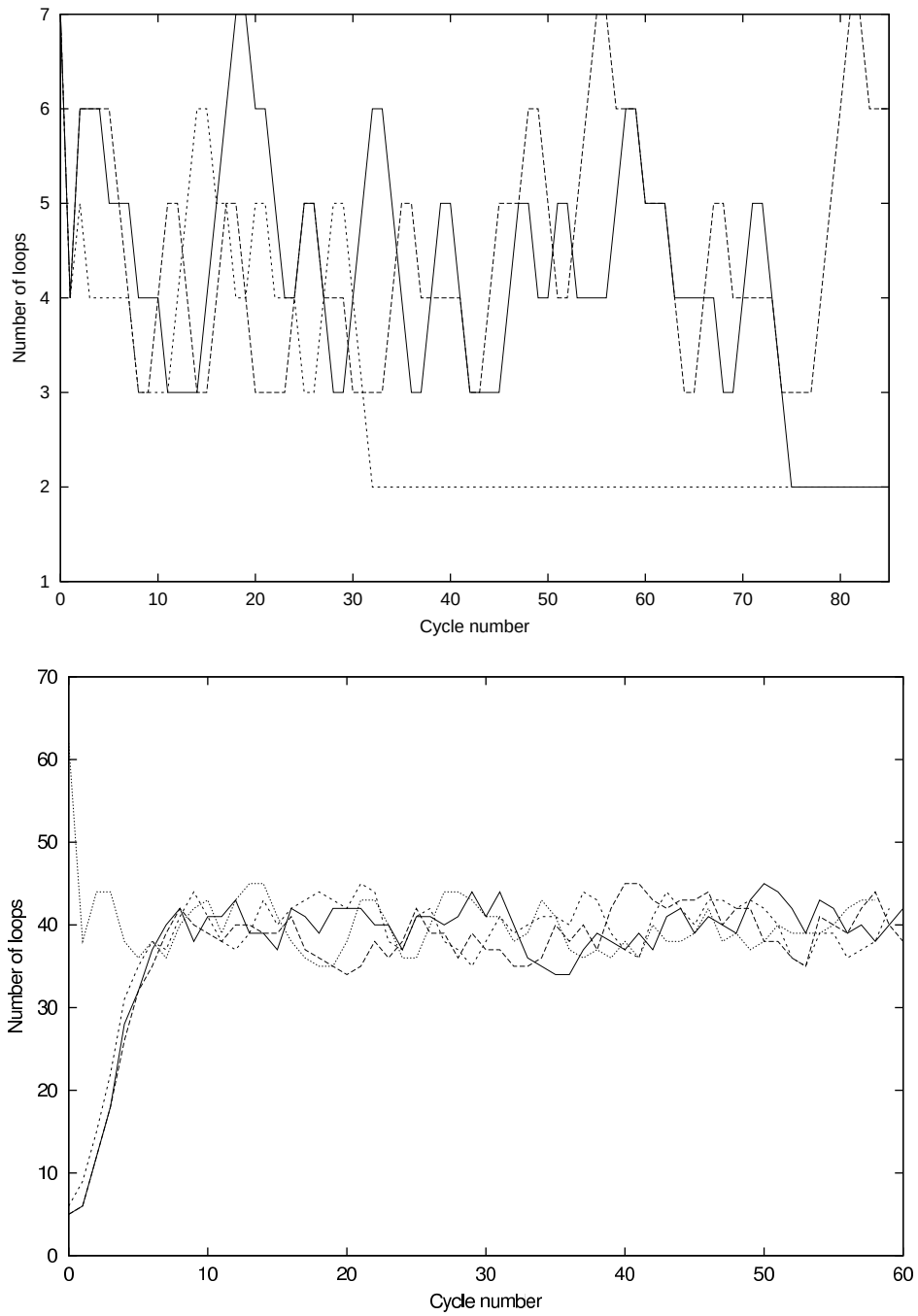

Figure 24: Numbers of loops around each sub-cycle for typical trajectories in the regular and irregular cases. $c = 1.0$, $e = 0.5$, $s_3 = 0.8$ in both cases. (a) Regular case: after transients two trajectories settle to $n = 2$ loops per sub-cycle, the third trajectory shown has not settled by cycle 80. $s_1 = 1.1$, $s_2 = 1.5$. (b) Irregular case: four different initial conditions converge to a bounded aperiodic sequence of loops. $s_1 = 1.0$, $s_2 = 1.4$.